Sewage sludge ash-derived materials for H2S removal from a landfill biogas

Valentine Gasquet, Boram Kim, Anne Bonhomme, Hassen Benbelkacem

▶ **To cite this version:**

Valentine Gasquet, Boram Kim, Anne Bonhomme, Hassen Benbelkacem. Sewage sludge ash-derived materials for H2S removal from a landfill biogas. Waste Management, 2021, 136, pp.230-237. 10.1016/j.wasman.2021.10.023 . hal-04185197

HAL Id: hal-04185197
https://hal.science/hal-04185197v1

Submitted on 5 Jan 2024

HAL is a multi-disciplinary open access archive for the deposit and dissemination of scientific research documents, whether they are published or not. The documents may come from teaching and research institutions in France or abroad, or from public or private research centers.

L'archive ouverte pluridisciplinaire **HAL**, est destinée au dépôt et à la diffusion de documents scientifiques de niveau recherche, publiés ou non, émanant des établissements d'enseignement et de recherche français ou étrangers, des laboratoires publics ou privés.

Distributed under a Creative Commons Attribution - NonCommercial 4.0 International License

Version of Record: https://www.sciencedirect.com/science/article/pii/S0956053X21005638
Manuscript_b47ba2cb3da205b84dfc757e09320a2d

Sewage Sludge Ash-derived materials for H_2S removal from a landfill biogas

GASQUET Valentine[1], KIM Boram[1,*], BONHOMME Anne[2], BENBELKACEM Hassen[1]

[1] *Univ Lyon, INSA Lyon, DEEP, EA 7429, 69621 Villeurbanne cedex, France*

[2] *IRCELYON, 6 rue Victor Grignard, F-69100 VILLEURBANNE, France*

[*] Corresponding author email: boram.kim@insa-lyon.fr

Abstract

H_2S removal is a key step for biogas cleaning because this component can lead to premature corrosion of the equipment and its cleaning has a significant cost. The aim of the present work was to assess the use of sewage sludge derived ash (SSA)-materials for H_2S removal from a landfill biogas. SSA and mixtures made with SSA, activated carbon (AC) and sand were tested for H_2S removal. The best removal efficiency was obtained with the mixture 80%m SSA and 20%m AC, while SSA alone was not a good adsorbent under tested experimental conditions. The materials characterization helped the adsorption mechanism understanding. Indeed, results highlighted that SSA presence stabilizes the pH on a basic range, favorable for H_2S dissociation into HS^- then its chemisorption. On the other hand, with the microporosity of AC, the contact surface between H_2S and oxygen was sufficiently large for chemisorption kinetics. It also appeared that the mixture with sand and AC adorbs non selectively H_2S but also other volatile organic pollutants present in biogas. Contrariwise, with SSA/AC mixtures, H_2S seems to be selectively chemisorbed.

Keywords: Sewage sludge ash, Biogas, H_2S removal, adsorption

© 2021 published by Elsevier. This manuscript is made available under the CC BY NC user license
https://creativecommons.org/licenses/by-nc/4.0/

1. Introduction

Sewage sludge (SS) is a by-product of wastewater treatment. Its composition varies, as different processing operations are available, according to the nature of pollutions. In order to facilitate its deposit or valorization, this produced sludge has to be stabilized. Three methods are available: thermal, chemical and biological stabilization (Gutiérrez Ortiz *et al.*, 2014). The chosen treatment and stabilization conditions (temperature and gas nature for a thermal treatment for example) can affect characteristics of the materials.

A European directive (200/60/EC) adopted on October 23rd 2000 defined sludge not as a waste material but as a product of sewage treatment (European Parliament, Directive 2000/60/EC). The conurbations must monitor and report sewage treatments and sludge disposal (Kacprzak *et al.*, 2017). The European Parliament and Council Directive 2008/98/EC of November 19th 2008 states that a priority in SS management is its preparation in order to reuse, recycle or recover it in another form (European Parliament, Directive 2009/28/EC). In the next years, the amount of SS sent to landfills will be restricted regarding orientations given by the current regulations. Incineration is a common option for SS management to reduce its volume. Indeed, in European Union, approximatively 10 Mt dry mass of SS is produced each year, of which 22% is incinerated (Lynn *et al.*, 2015). In order to save resources and participate to circular economy, Sewage Sludge Ash (SSA) is partly recycled as a building material such as cement or concrete mortars, as an inert material in replacement of sand or as replacement of raw materials for light aggregates production (Lynn *et al.*, 2018).

On the other hand, another current issue is energy production and the limitation of CO_2 emissions. Renewable energy development is therefore necessary. Biogas is a renewable gas obtained by the anaerobic digestion of organic waste, such as SS. Biogas' advantages are its non-intermittence, the possibility to produce it locally (and consequently less transport) and its different uses. Indeed, biogas can be valorized for heat and power generation with a CHP unit, as a fuel for vehicles (compressed or liquefied) and injected into the gas grid, for domestic or industrial use.

Biogas must be cleaned because it contains many pollutants, in particular hydrogen sulfide (H_2S). Its concentration ranges from 10 to 10,000 ppm_v depending on the biogas origin. Currently, this pollutant can be removed with biological treatment, by adsorption on iron oxides/hydroxides or on impregnated activated carbon (Awe *et al.*, 2017). All these technologies have drawbacks and especially natural resources depletion. It is the reason why the possibility of adsorbing H_2S on alternative materials is studied Based on the literature, H_2S can be removed with mineral wool waste (Bergersen and Haarstad, 2014), basic oxygen furnace slag (Sarperi *et al.*, 2014), alum sludge (Ren *et al.*, 2020), municipal solid waste incineration bottom ash (del Valle-Zermeño *et al.*, 2015; Fontseré Obis *et al.*, 2017a) and also biochars (Shang *et al.*, 2013;2016; Bamdad *et al.*, 2018).

SS has been used as precursor for adsorbents production, after a pyrolysis (Bagreev *et al.*, 2001; Ros *et al.*, 2006; Gutiérrez Ortiz *et al.*, 2014). This thermal treatment develops the material porosity, with surface area going from 12 to 248 m²/g (Wallas *et al.*, 2014; Possa *et al.*, 2018). The pyrolyzed sludge contains 50-70% organic matter and is also enriched in metals such as iron, zinc and aluminum (Ros *et al.*, 2006). For H_2S removal, pyrolyzed sludge can also be impregnated with NaOH (Polruang *et al.*, 2017), with HCl (Possa *et al.*, 2018) or activated with CO_2 (Wallas *et al.*, 2014). Adsorption capacities until 183 mg_{H2S}/g_{DM} are obtained with pyrolyzed SS (Ros *et al.*, 2007). The adsorption results show that the pyrolysis temperature has a significant influence on removal capacities, with an adsorption capacity going from 14.9 to 82.6 mg_{H2S}/g_{DM} for the same sludge pyrolyzed respectively at 600 and 950°C. However, most of these studies are realized with air or synthetic biogas and not with a real and complex biogas. Furthermore, no study has been reported on the use of SSA for H_2S adsorption. The main difference between SS biochars and SSA is the porosity, very low for SSA unlike the biochars' one. Adsorption is a surface mechanism and can be limited by a low porosity.

Some studies deal with H_2S adsorption using formulated materials, associating an alternative material and activated carbon (AC) in order to use its porosity. Florent *et al.* worked on materials made from SS and AC pyrolyzed together at 600 or 800°C (Florent *et al.*, 2019). Mixtures containing 10 and 30% of AC are three times more efficient for H_2S removal than the sludge pyrolyzed alone, with a final

adsorption capacity of 22 mg_{H2S}/g. The authors indicate that the porosity contribution leads to a better availability of catalytic centers linked with H_2S oxidation. Sioukri *et al.* (2005) observed an evolution of the theoretical and real adsorption capacity from 30 to 80 mg_{H2S}/g with a mixture SS/AC pyrolyzed at 950°C. The developed pore system is used to store the oxidation products of H_2S removal. Therefore, it seems interesting to add AC to SSA in order to obtain a good adsorbent for H_2S.

The objective of this work is to estimate the potential of SSA itself and SSA blended with AC as adsorbent for H_2S removal from a real landfill biogas and to understand related adsorption mechanisms.

2. Materials and methods

2.1. Materials

SSA was collected from a wastewater treatment plant situated in the southeast part of France. SSA was obtained by combustion of urban SS (a mix of primary and secondary sludge) in a fluidized bed furnace at 900°C and recovered from the fumes thanks to an electrostatic precipitator. SSA contains 30% SiO_2, 23% CaO, 16% P_2O_5, 10% Al_2O_3, and 7% Fe_2O_3 (low loss-on-ignition, 5%). The high amount of phosphoric oxide can be explained by dephosphatation in wastewater treatment plant. No pretreatments were realized on the ash due to its particle size (< 100 µm). AC used for adsorption tests is the Pulsorb 208CP, produced by Chemviron, a Kuraray branch. It was obtained by coconut shells carbonization, activated with vapor and ground in powder form. The supplier indicates a surface area of 1200 m^2/g. A sand was also used as an inert additive to AC compare to SSA for H_2S adsorption. It is produced by Sibelco (ref. HN31) and composed of 98.9% of silica.

Primary test showed that the adsorption efficiency increases with humidity (result not shown here). For adsorption experiment, SSA was humidified at 20%m. Distilled water was slowly added to the raw material with a continuous stirring. Mixtures were realized by mixing SSA or sand with AC in percentage of mass. The water contents of all mixtures were adjusted to 15-20% w/w which is

considered as optimal water contents for better H_2S adsorption according to the previous study (Fontseré *et al.,* 2017b), highlighting water influence of H_2S adsorption.

Four different samples were prepared for adsorption test comparing: SSA alone, two mixtures of SSA with AC (10%m and 20%m of AC) and a mixture of sand with 20%m of AC. Subsequently, to lighten the text, these studied samples will be respectively called: SL (SSA alone), SLA10 (SSA with 10%m of AC), SLA20 (SSA with 20%m of AC) and SDA20 (sand with 20%m of AC).

2.2. Biogas adsorption tests

The experimental set-up for biogas adsorption tests was described previously (Gasquet *et al.*, 2020) and the diagram is presented on the Figure 1. To summarize, experiments were realized on a landfill, using a real biogas. Consequently, the inlet biogas composition did not stay constant for all the tests. The mean H_2S concentration ranged between 1415 to 1715 ppm_v, as observed in Table 1. Indeed, depending on the grid management, some air can be introduced in the biogas and diluted it. Moreover, for the same reason, H_2S concentration can reach 5000 ppm_v during a short period. These variations may have an influence on the amount of H_2S captured and it is therefore important to consider it. The tests were not realized simultaneously and the biogas mean temperature was around 21°C.

A reactor of 24.5 cm high and a diameter of 4 cm was used. The material volume was constant for all experiments (251 cm^3), with a fixed height in the reactor equal to 20 cm. This is the reason why the mass of dry sample was different for each case, with different densities, from 0.9 for SL to 2.65 for SDA20 (see Table 1). Hence, the AC mass was different for each test, with respectively 11.4, 21.9 and 44.9 g for SLA10, SLA20 and SDA20. The biogas flow was fixed at 1 L/min, using a Ritter volumetric flowmeter. Residence time in the reactor was therefore equal to 15 seconds. Biogas composition was analyzed with an infrared laser spectrometer called ProCeas. Biogas bubbles in a vial containing water before the reactor to humidify it.

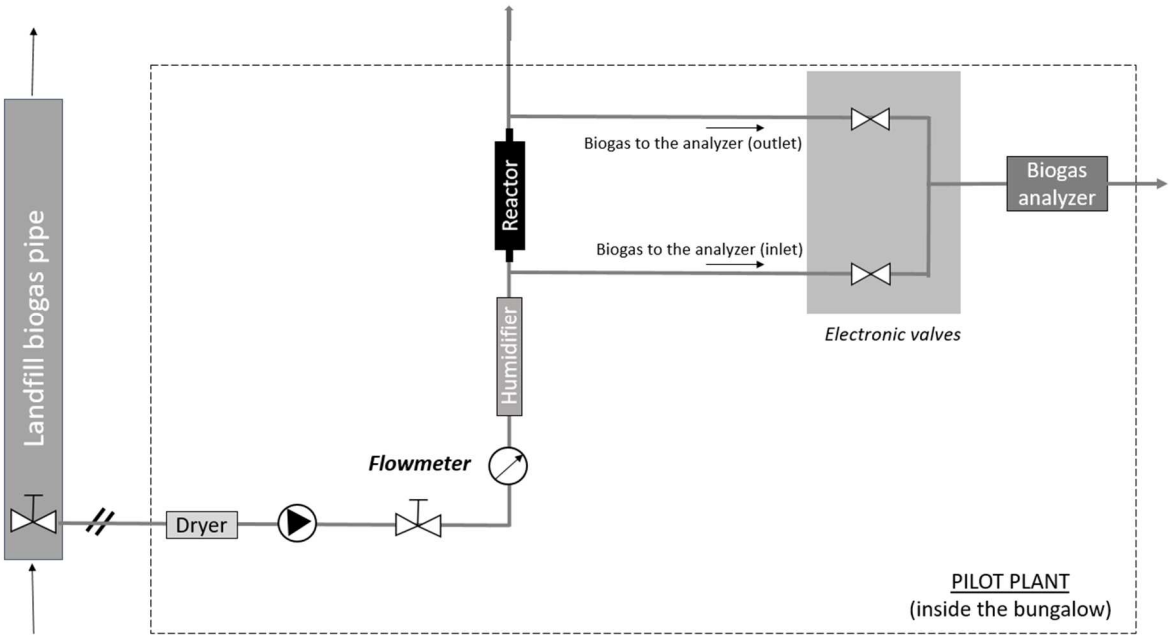

Figure 1 : Lab-scale adsorption pilot

In order to compare the materials, some parameters are calculated. First, H_2S_{passed} and $H_2S_{captured}$ are calculated as presented in equations (1) and (2), with $[H_2S]_{inlet}$ and $[H_2S]_{outlet}$ respectively the inlet and outlet H_2S concentration in g/m^3. $\dot{V}$ represents the gas flow in m^3/min. Mass adsorption capacity is obtained by dividing the H_2S amount removed by the dry mass of the adsorbent. The H_2S amount captured at which point the ratio $[H_2S]_{outlet}/[H_2S]_{inlet}$ is equal to 0.1 (10%) is also compared for the materials.

$$H_2S_{passed} = \int_0^t [H_2S]_{inlet}(t) \times \dot{V}\,(t)\,dt \quad (1)$$

$$H_2S_{captured} = \int_0^t ([H_2S]_{inlet}(t) - [H_2S]_{outlet}(t)) \times \dot{V}\,(t)\,dt \quad (2)$$

146 **Table 1: Summary of experimental conditions of adsorption tests for SSA derived materials**

Material	Duration (days)	Flow (L/min)	[H_2S] inlet (ppm_v)	Temperature (°C)	Masse of dry sample (g)
SL	7	1.05	1415 ± 605	20.3 ± 1.9	138.6
SLA10	10	0.97	1445 ± 255	20.1 ± 1.1	114.2
SLA20	8	1.03	1680 ± 780	21.0 ± 1.7	109.7
SDA20	7	0.95	1715 ± 825	21.0 ± 1.4	224.3

147

148 ***2.3. Materials characterization***

149 To compare physicochemical characteristics between different materials but also to better understand
150 H_2S adsorption mechanisms, following analyses were performed.

151

152 Water content was measured by drying the material at 105°C during 24 hours in a Memmert oven. All
153 analyses were carried out in triplicate with 20-30 g of sample. Surface area and porous volume were
154 measured by nitrogen adsorption at 77 K using ASAP 2020 device from Micromeritics. The surface
155 area was evaluated with the Brunauer Emmett Teller (BET) model using the software MicroActive
156 from Micrometrics. The porous volume was calculated with the Saieus software from Micrometrics,
157 applying the NLDFT model "Carbon 2D Heterogeneous Surface". This method allows the
158 characterization of the micro (< 2 nm) and mesoporosity (between 2 and 50 nm).

159

160 pH was measured with a calibrated pH-meter (Consort C3431) after 48 h leaching with distilled water,
161 based on the ANC 14429 norm. CHNS composition was determined with a FlashEA 1112 Series
162 analyzer from ThermoFischer. The major element (with a concentration higher than 10 g/kg)
163 compositions were determined with Inductively Coupled Plasma Atomic Emission Spectroscopy (ICP-
164 OES, Thermo Fischer Icap 6500) after sample fusion with $LiBO_2$ followed by dissolution using HNO_3.

165

166 Raman spectroscopy was realized at room temperature under air with a Kaiser RXN1 and a Charged-
167 Coupled Device of the same brand. Spectra were obtained with an excitation laser working at a
168 wavelength of 785 nm. The acquisition spectral region goes from 100 to 3420 cm^{-1} with a resolution of
169 4 cm^{-1}. Pyrolysis with Gas Chromatography-Mass Spectroscopy (Pyro GC-MS) consists of an analysis

of the gaseous components produced during a flash pyrolysis, at 550°C. 1 to 2 mg of sample was introduced in the pyrolyzer (EGA/Py-3030D model from Frontier Lab) at the desired temperature under inert gas (He). The pyrolysis gas was drawn to the chromatography column (HP-5ms). After this column, the mass spectrometer (simple quadrupole model 5977B from Agilent) detects the components depending on the ratio mass to charge (m/z).

3. Results

3.1. Comparison of H_2S removal efficiencies

On the Figure 2, the evolution of the ratio $[H_2S]_{outlet}$ over $[H_2S]_{inlet}$ also called C/C_0 is observed as a function of the time for the SL, SLA10, SLA20 and SDA20.

First, it appears that SL had quite different behaviors compared to other materials. The immediate breakthrough shows that the adsorbent never removes all the H_2S from the biogas. More than 80% of the inlet H_2S was found at the outlet of the reactor, around 1100 ppm_v. The ratio C/C_0 remained constant during the entire test. Therefore, this material can remove a constant (low) amount of H_2S during around one week. Adsorption mechanisms take place but not sufficiently to use SL as an effective adsorbent for H_2S.

The three materials containing AC could remove all H_2S during the first day. The breakthrough was first observed for SLA10 after one day, and then for SDA20 after 1.7 days. Finally the last breakthrough was observed for SLA20 (2.7 days). The curve slope was not either the same, with a steeper slope for SDA20. This material reached faster its total saturation. A peak was observed for SLA10 at 2.8 days. It can be explained by a quick rise of H_2S inlet concentration (5000 ppm_v) due to the landfill grid management. At this point, inlet H_2S amount was too high for materials to adsorb the same H_2S fraction than the one adsorbed when H_2S inlet concentration was 1500 ppm_v. Finally, after 6 days, all materials removed less than 25% of the inlet H_2S.

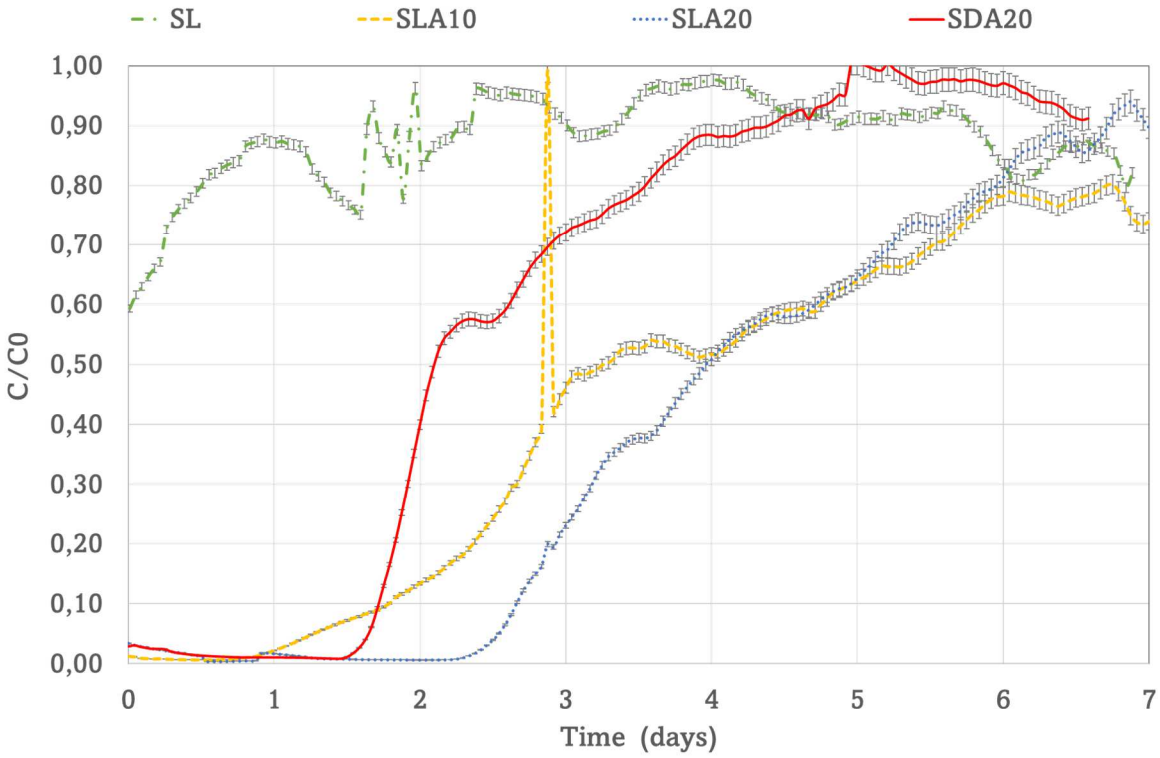

Figure 2: Evolution of C/C_0 as a function of the time for SSA derived materials

The main adsorption results are summarized in Table 2. The total H_2S amounts passed and captured are presented. The ratio $H_2S_{captured}/H_2S_{passed}$ is also calculated. It evolved from 0.14 for SL to 0.56 for SLA20. It means that more than half of the total H_2S amount passed in the reactor was captured for SLA20. This ratio was lower for SDA20 (0.37) and equal to 0.33 for SLA10.

The 10% breakthrough was reached practically at the same time (1.8 days) for SLA10 and SDA20. This result was also observed on the Figure 2, when the curves intersect, even if the forms are different.

The material with the lower final mass adsorption capacity was SL (Table 2), followed by SDA20 with respectively 22 and 39 mg_{H2S}/g_{DM}, which is half the value for SLA10 (87 mg_{H2S}/g_{DM}). The highest final mass adsorption capacity was obtained for SLA20 with 186 mg_{H2S}/g_{DM}.

As the blended AC masses within materials for each test were different, total H_2S captured can then be expressed according to AC masses to compare adsorption efficiencies of tested mixed materials. This value went from 190 to 800 mg_{H2S}/g_{AC} respectively for SDA20 and SLA10. It is equal to 720 mg_{H2S}/g_{AC} for SLA20 . Then, it appeared that there was a created synergy between AC and SSA.

Table 2: Synthesis of the adsorption results of mixtures

	SL	SLA10	SLA20	SDA20
Total H_2S passed (g)	22.9 ± 1.1	30.3 ± 1.5	29.2 ± 1.5	23.6 ± 1.2
Total H_2S captured (g)	3.1 ± 0.2	10.0 ± 0.5	16.4 ± 0.8	8.7 ± 0.4
H_2S captured / H_2S passed (g/g)	0.14 ± 0.01	0.33 ± 0.02	0.56 ± 0.03	0.37 ± 0.02
10% breakthrough time (days)	-	1.8	2.7	1.8
Final adsorption capacity (mass) at the end of the test (mg_{H2S}/g_{DM})	22 ± 1	87 ± 4	186 ± 9	39 ± 2

3.2. Characterization of raw and used materials

The materials were characterized before and after adsorption tests to better understand adsorption mechanisms taking place for each one.

3.2.1.pH, water content and sulfur content

SL and AC initial pH were respectively 11.4 and 10.4 (Table 3). For the SSA-based mixtures, pH went from 9.8 for SLA20 to 10.4 for SLA10. pH of SDA20 was equal to 10.4. All adsorbents were therefore basic. After adsorption tests, pH decreased for all materials. While the pH for mixtures containing SSA seemed to stabilize around 8, the pH of SDA20 fell to 2.7, becoming very acid, which must probably be limiting for H_2S chemisorption. Indeed, H_2S dissociation into HS^- can take place only if the pH ranges between 7.2 and 12.9. This pH sharp drop can be explained by the absence of buffer capacity for the mixture SDA20. Therefore, SSA presence is useful for stabilizing pH in a basic range, suitable for H_2S dissociation.

All materials were dried after adsorption (see Table 3). SL lost 8% of humidity. For mixed materials, humidity remained higher than 10%. It suggests that water content was not a limiting factor for H_2S

adsorption. The mixture SDA20 dried slightly less than the mixture with SSA, as its initial water content was lower. It can be linked with the fact that sample mass in the reactor for SDA20 was higher and consequently the water mass was also higher at the beginning of the experimental test (34 g of water for SDA20 against 23 g for SLA20).

Sulfur content measured with CHNS analysis was also presented in the Table 3 for raw and used materials. The lowest increase of sulfur amount was remarked for SL with 2.4%S. It was consistent with H_2S mass adsorption capacity equal to 2.2%. The highest sulfur amount was measured for SLA20 with 16%S for the used material and an increase of 14.4%. It was a bit lower than the mass adsorption capacity. Sulfur amounts and mass adsorption capacities were also consistent for SLA10 and SDA20.

Table 3: Evolution of pH, water content, sulfur content, surface area, microporous volume and mesoporous volume of materials before and after adsorption

[before / after] adsorption	SL	SLA10	SLA20	SDA20
pH	11.4 ± 0.6 / 8.3 ± 0.4	10.4 ± 0.5 / 8.1 ± 0.4	9.8 ± 0.5 / 8.0 ± 0.4	10.2 ± 0.5 / 2.7 ± 0.4
Humidity (%)	19.5 ± 1.0 / 11.5 ± 0.6	20.5 ± 1.0 / 12.5 ± 0.6	20.0 ± 1.0 / 15.0 ± 0.8	15.0 ± 0.8 / 12.0 ± 0.6
Sulfur content (%)	1.4 ± 0.1 / 3.8 ± 0.2	1.6 ± 0.1 / 9.2 ± 0.5	1.7 ± 0.1 / 14.4 ± 0.7	0.5 ± 0.1 / 5.2 ± 0.3
Surface area ($m^2.g^{-1}$)	7 / 9	130 / 5	215 / 5	245 / 14
Microporous volume ($cm^3.g^{-1}$)	0.000 / 0.000	0.048 / 0.000	0.082 / 0.000	0.095 / 0.004
Mesoporous volume ($cm^3.g^{-1}$)	0.040 / 0.050	0.058 / 0.040	0.057 / 0.035	0.012 / 0.009

3.2.2.Porosity

SL had very low surface area, equal to 7 m²/g (see Table 3). The surface area of the commercial AC was 1200 m²/g. Surface areas of the mixtures were roughly equal to the weighted addition of each surface area of mixed raw materials. Indeed, surface areas of SLA20 and SLA10 were respectively equal to 215 and 130 m²/g. SDA20 had a surface area slightly higher than the mixture with SSA, with 245 m²/g.

Regarding meso- and micropore volumes (Table 3), the total porosity of SL can be mainly represented by mesopores, with a volume of 0.040 cm^3/g. AC addition brought micropores: 0.082 cm^3/g for SLA20 and 0.048 cm^3/g for SLA10. These mixtures also contained mesopores from SSA, respectively 0.057 and 0.058 cm^3/g. The mixture with sand had less mesopores (0.012 cm^3/g) which suggests that AC was mainly microporous.

The evolution of micro and mesoporosity as well as surface area are presented in Table 3. The first observation was that the porosity and the surface area of SL did not evolve after adsorption. For other materials, the surface area decreased drastically. Mesoporous volume also decreased but more particularly for SSA-based mixtures, as the initial mesoporous volume of SDA20 was already low. Mesopores seemed therefore implied in H_2S adsorption.

Concerning microporous volume, it was almost null after adsorption for all materials, no matter what their initial values. H_2S adsorption was therefore related to microporous saturation. The volume loss was however not proportional to the amount of H_2S adsorbed. Indeed, SDA20 lost 0.090 cm^3/g of microporous volume while it retained 8 g of H_2S. On the other hand, SLA20 lost 0.082 cm^3/g of micropores with 16.4 g of H_2S captured. Physisorption was therefore not the only explanation for H_2S removal with these mixtures. Florent *et al.* also observed a steep decrease of the microporous volume after adsorption for pyrolyzed mixtures composed of SS and AC (Florent *et al.*, 2019). Authors said that adsorption stops when all pores are filled with sulfur.

3.2.3. Raman spectroscopy

Based on the literature, Raman spectroscopy can be used to validate elemental sulfur presence in adsorbents (Piergrossi *et al.*, 2019). Piergrossi *et al.* observed that sulfur Raman peaks overlap with the ones of AC having adsorbed sulfur.

As two mixtures contain SSA and AC but in different proportions (SLA10 and SLA20), only SLA20 was analyzed by Raman spectroscopy. Regarding SL, its adsorption capacity was only 22 mg_{H2S}/g_{DM} difficult to be quantified by analytical methods. It is the reason why another material was analyzed thereafter: SL-25days. This material was the same than SL but the adsorption test lasted 25 days instead of 7 days. Final mass adsorption capacity was equal to 74 mg_{H2S}/g_{DM}.

Raw and used materials were analyzed by Raman spectroscopy, as well as elemental sulfur. No significant peaks were observed for raw materials and it was the reason why the spectra were not presented. The spectra for elemental sulfur, SL-25days, SLA20 and SDA20 after adsorption were presented on the Figure 3. Three main peaks related to elemental sulfur were observed, at 152, 218 and 472 cm^{-1}. These peaks were also found for SL-25days and SLA20. This observation attested sulfur presence in these materials. During adsorption, H_2S was therefore transformed into elemental sulfur.

On the other hand, no peak was observed for SDA20 even though its adsorption capacity was 39 mg_{H2S}/g_{DM} (non-negligible), corresponding to 34 mg_{H2S}/cm^3. Preliminary analyses performed in the laboratory showed that the detection limit of elementary sulfur by Raman spectroscopy was between 18 and 40 mg_{H2S}/cm^3. It may suggest that adsorbed H_2S on SDA20 was not all transformed into S_8 by chemisorption processes.

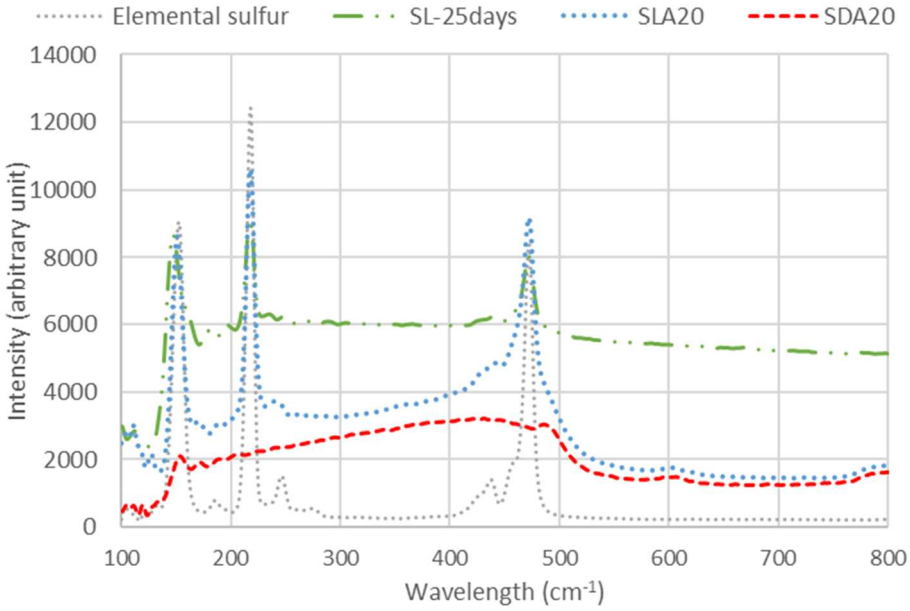

Figure 3: Raman spectra of elemental sulfur, SL-25days, SLA20 and SDA20

3.2.4.Pyro GC-MS

Pyro GC-MS analyses results cannot be quantitatively interpreted but could be qualitatively commented regarding organic compounds within different raw and used materials (Figure 4). In raw materials, few presences of volatile organic compounds were observed. Only benzene and toluene were measured in SLA20, SLA10 and SDA20. After adsorption tests, several volatile organic compounds were observed with SDA20, such as toluene, ethylbenzene or xylene (Figure 4). They were also identified in the material made from SLA20 and SLA10 but in lower amounts. These compounds could be observed by thermal decompositions of volatile organic compounds from landfill biogas. No volatile organic compounds were identified in SL-25days. While SDA20 adsorbed less sulfur than SLA20, the material retained more quantity of volatile organic compounds. This observation confirmed that AC adsorption was non-selective.

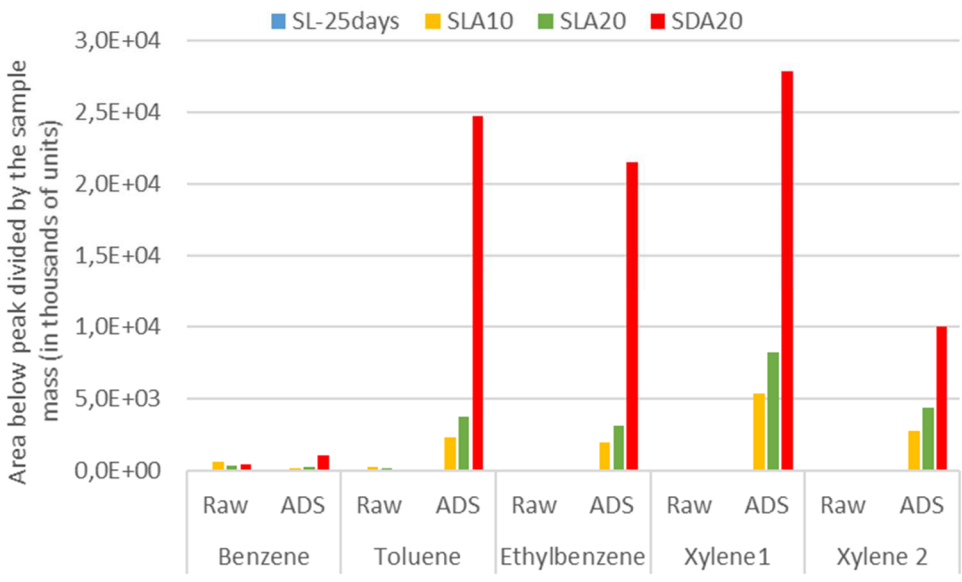

Figure 4: Organic components content by Pyro GC-MS results for SL-25days, SLA10, SLA20 and SDA20

3.3. Adsorption mechanisms

Materials characterization before and after H_2S adsorption provided further information about adsorption phenomena taking place within studied materials. Their adsorption mechanisms are graphically synthetized on the Figure 5.

In the literature concerning H_2S retention with impregnated activated carbon, it is indicated that H_2S is removed via chemisorption. Indeed, if the material is basic (pH between 7.2 and 12.9), H_2S is dissociated into HS^- and then oxidized into elemental sulfur (Bagreev and Bandosz, 2005; Xiao *et al.*, 2008). The larger the porosity, the more molecules can be captured (Bagreev and Bandosz, 2002). Physisorption can also take place for H_2S removal but with slower kinetics.

SL contained oxygenated site and catalyst minerals that can promote chemisorption of H_2S (Nguyen-Thanh and Bandosz, 2005) as described before. As the material was previously humidified, water films surround pores. SL captured around 2% sulfur and could not retain more than 20% of the inlet H_2S during the entire adsorption test. However, after one week, SL still adsorbed a little amount of H_2S. SL had extremely low porosity, composed only of mesopores. This porosity did not evolve after adsorption. Therefore, it seemed that the absence of micropores was the limiting factor for H_2S adsorption on SL.

On Figure 5, SLA20 is drawn with grey grains representing SSA and pink grains representing AC. As well as SL, a water film is present. The porosity is larger here with the presence of microporosity.

SLA20 showed the highest mass adsorption capacity, with 186 mg_{H2S}/g_{DM}. Adsorption was efficient because SLA20 had suitable characteristic. First, SLA20 had mesopores from SSA and micropores brought by AC. In the literature, micropores were considered as nanoreactors for H_2S dissociation and oxidation (Surra *et al.*, 2019). These micropores create reactional sites between HS^- and oxygen. During adsorption, micropores were progressively filled, as observed previously in Table 3 with the decrease of the micropores volume from 0.083 cm^3/g to almost zero. The surface area of the material was therefore high enough for H_2S chemisorption. Some organic compounds could nevertheless be adsorbed in micropores. On the other hand, SLA20 maintained basic pH at the end of the test thanks to its buffer capacity. H_2S dissociation was then not limited by pH. Besides, elemental sulfur was observed in SLA20-ADS with Raman spectroscopy and Pyro GC-MS, confirming H_2S chemisorption. By Sioukri *et al.*, synergy between AC and SSA was reported thanks to the combined presence of small pores (around 1 nm) and catalytic centers (Sioukri *et al.*, 2005). It would favor as-formed sulfur retention, filling progressively all the porous volume. However, the porous network must be sufficiently interconnected to make the small pores easily available.

343 CHNS analysis indicated that SDA20 contains 5.2% of sulfur after adsorption test. According to
344 characterization results, it seemed that SDA20 adsorption takes place in several steps. At the
345 beginning of the test, SDA20 was wet (15 % w/w of humidity) and the pH was basic (10.4). With
346 these conditions, H_2S dissociated into HS^- then oxidized into elemental sulfur thanks to oxygen
347 presence within biogas. However, SDA20 had no buffer capacity so could not maintain basic pH until
348 the end of adsorption tests. pH decreased quickly due to the contact with acid gas (H_2S and CO_2), yet
349 when pH is below seven, H_2S can be only physisorbed. Moreover, the significant presence of
350 elemental sulfur was not observed with Raman spectroscopy within SDA20, suggesting that H_2S may
351 not be mainly adsorbed under elemental sulfur form within this material. Indeed, a pH of 2.7 was
352 certainly due to the acid sulfuric formation. Non-selective physisorption can also take place
353 simultaneously. Landfill biogas organic compounds were identified in significant amounts by pyro
354 GC-MS within SDA20. These compounds were represented with a blue square on the drawing on the
355 Figure 5. Microporosity was the main driver of this physisorption. Indeed, at the end of adsorption
356 tests, SDA20 micropore volume was almost null while it was equal to 0.095 cm^3/g for the raw sample.
357

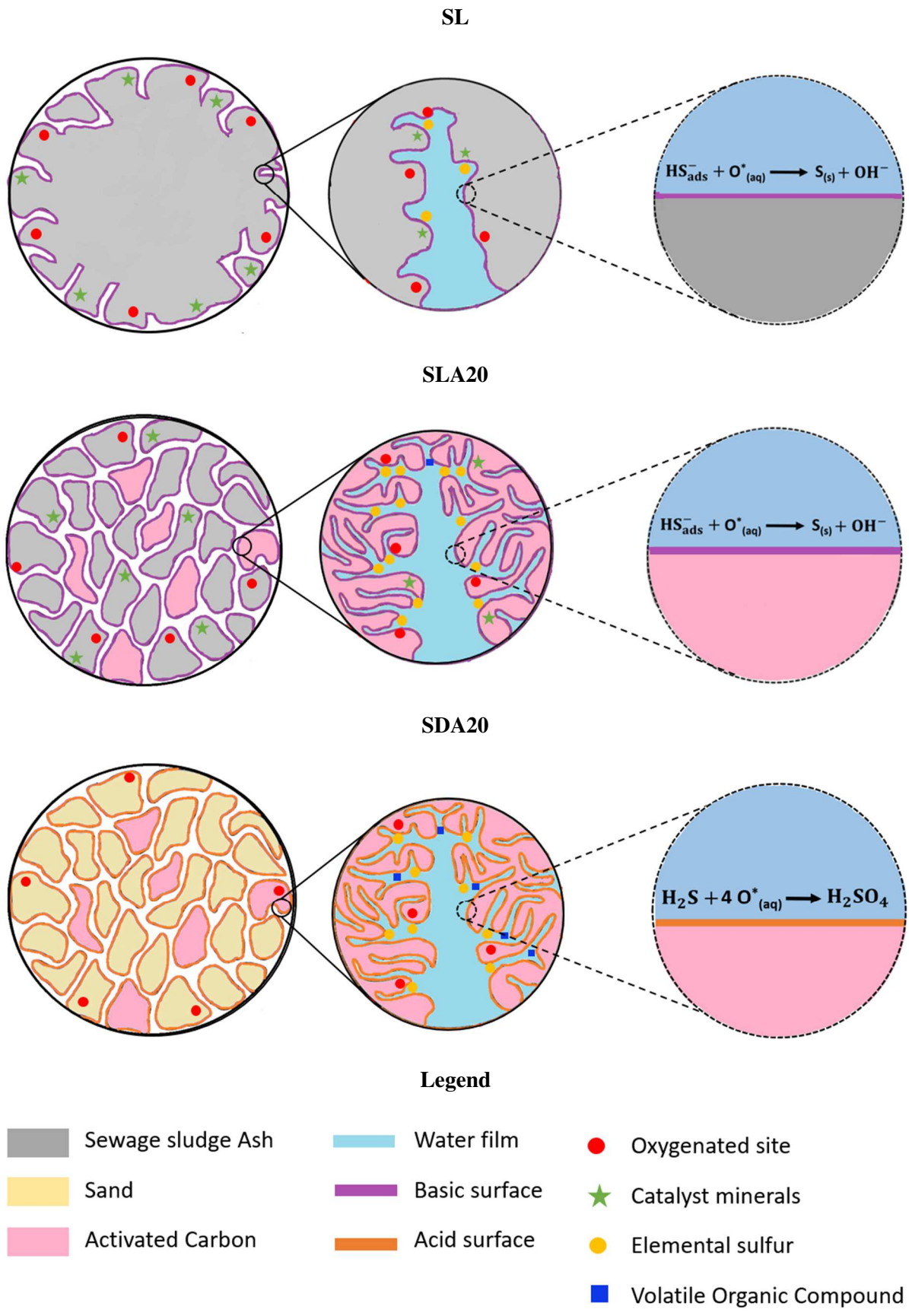

358 **Figure 5: Schematic mechanisms with each material**

359

4. Conclusions

The adsorption tests during this study highlighted interesting potential of SSA when it was mixed with AC for H_2S removal. Indeed, removal capacities of the material are significantly improved, even if only 10% of AC was added. For a same amount of H_2S passed, SSA adsorbs 22 mg_{H2S}/g_{DM} while SLA10 retains two times more H_2S and SLA20 five times more. Besides, these mixtures capture the whole H_2S entering during the first day of the adsorption test which was not the case for SSA. It is an important feature for using these materials as H_2S adsorbents at industrial scale

Comparing sand/AC mixture test with SSA/AC mixtures test showed that good H_2S adsorption capacity for mixture SSA/AC was due to a synergy of both materials, having complementary physicochemical characteristics and not only an improvement of adsorption capacity. SSA can then be seen as a “low cost” impregnated material to improve the AC adsorption capacity. More than that, in order to save resources and participate to circular economy, mixing SSA with a porous material is a promising way to valorize SSA and to reduce energy production costs from biogas.

Acknowledgements

The authors are grateful for the fnancial support provided by the Agence de l’Eau Rhône Méditerranée Corse (VALBIFIL project). They also thank Hervé Perier-Camby and Richard Poncet (DEEP laboratory– INSA Lyon, France) for their technical support. This work was performed within the framework of the EUR H2O’Lyon (ANR-17-EURE-0018) of Université de Lyon (UdL), within the program "Investissements d'Avenir” operated by the French National Research Agency (ANR).

Bibliography

Awe O. W., Zhao Y., Nzihou A., Minh D. P., and Lyczko N., 2007. A Review of Biogas Utilisation, Purification and Upgrading Technologies, Waste Biomass Valorization, 8, 267-283.

Bagreev A., Bashkova S., Locke D. C., and Bandosz T. J., 2001. Sewage Sludge-Derived Materials as Efficient Adsorbents for Removal of Hydrogen Sulfide, Environ. Sci. Technol., 35, 1537-1543.

Bagreev A. and Bandosz T. J., 2002. H_2S Adsorption/Oxidation on Materials Obtained Using Sulfuric Acid Activation of Sewage Sludge-Derived Fertilizer, J. Colloid Interface Sci., 252, 188-194.

Bagreev A. and Bandosz T. J., 2005. On the Mechanism of Hydrogen Sulfide Removal from Moist Air on Catalytic Carbonaceous Adsorbents, Ind. Eng. Chem. Res., 44, 530-538.

Bamdad H., Hawboldt K., and MacQuarrie S., 2018. A review on common adsorbents for acid gases removal: Focus on biochar, Renew. Sustain. Energy Rev., 81, 1705-1720.

Bergersen O. and Haarstad K., 2014. Treating landfill gas hydrogen sulphide with mineral wool waste (MWW) and rod mill waste (RMW), Waste Manag., 34, 141-147.

del Valle-Zermeño R., Romero-Güiza M. S., Chimenos J. M., Formosa J., Mata-Alvarez J., and Astals S., 2015. Biogas upgrading using MSWI bottom ash: An integrated municipal solid waste management, Renew. Energy, 80, 184-189.

Florent M., Policicchio A., Niewiadomski S., and Bandosz T. J., 2019. Exploring the options for the improvement of H_2S adsorption on sludge derived adsorbents: Building the composite with porous carbons, J. Clean. Prod., 119412.

Fontseré Obis M., Germain P., Bouzahzah H., Richioud A., and Benbelkacem H., 2017a. The effect of the origin of MSWI bottom ash on the H_2S elimination from landfill biogas, Waste Manag., 70, 158-169.

Fontseré Obis M., Germain P., Troesch O., Spillemaecker M., and Benbelkacem H., 2017b. Valorization of MSWI bottom ash for biogas desulfurization: Influence of biogas water content, Waste Manag., 60, 388-396.

Gasquet V., Kim B., Sigot L., and Benbelkacem H., 2020. H_2S Adsorption from Biogas with Thermal Treatment Residues, Waste Biomass Valorization, 11, 5363-5373.

Gutiérrez Ortiz F. J., Aguilera P. G., and Ollero P., 2014. Biogas desulfurization by adsorption on thermally treated sewage-sludge, Sep. Purif. Technol., 123, 200-213.

Kacprzak M. , Neczaj E., Fijałkowski K., Grobelak A., Grosser A., Worwag M., Rorat A., Brattebo H., Almås A., and Singh B. R., 2017. Sewage sludge disposal strategies for sustainable development, Environ. Res., 156, 39-46.

Lynn C. J., Dhir R. K., Ghataora G. S., and West R. P., 2015. Sewage sludge ash characteristics and potential for use in concrete, Constr. Build. Mater., 98, 767-779.

Lynn C. J., Dhir R. K., and Ghataora G. S., 2018. Environmental impacts of sewage sludge ash in construction: Leaching assessment, Resour. Conserv. Recycl., 136, 306-314.

Nakic D., 2018. Environmental evaluation of concrete with sewage sludge ash based on LCA, Sustain. Prod. Consum., 16, 193-201.

Nguyen-Thanh D., Bandosz T.J., 2005. Activated carbons with metal containing bentonite binders as adsorbents of hydrogen sulfide, Carbon, 43, 359-367.

Pavlík Z. , Fořt J., Záleská M., Pavlíková M., Trník A., Medved I., Keppert M., Koutsoukos P. G., and Černý R., 2016. Energy-efficient thermal treatment of sewage sludge for its application in blended cements, J. Clean. Prod., 112, 409-419.

Piergrossi V., Fasolato C., Capitani F., Monteleone G., Postorino P., and Gislon P., 2019. Application of Raman spectroscopy in chemical investigation of impregnated activated carbon spent in hydrogen sulfide removal process, Int. J. Environ. Sci. Technol., 16, 1227-1238.

Polruang S., Banjerdkij P., and Sirivittayapakorn S., 2017. Use of Drinking Water Sludge as Adsorbent for H2S Gas Removal from Biogas, EnvironmentAsia, 10, 1.

Possa R. D., Sousa J. F., Oliveira J. A., Nascimento P. F., Lima M. A. B., Brandão I., and Bezerra M. B. D., 2018. Dynamic adsorption of H2S in a fixed bed of sewage sludge pyrolysis char, Brazilian Journal of Petroleum and Gas, 12, 77-90.

Ren B., Lyczko N., Zhao Y., and Nzihou A., 2020. Alum sludge as an efficient sorbent for hydrogen sulfide removal: Experimental, mechanisms and modeling studies, Chemosphere, 248, 126010.

Ros A., Montes-Moran M. A., Fuente E., Nevskaia D. M., and Martin M. J., 2006. Dried Sludges and Sludge-Based Chars for H_2S Removal at Low Temperature: Influence of Sewage Sludge Characteristics, Environ. Sci. Technol., 40, 302-309.

Ros A., Lillo-Ródenas A., Canals-Batlle C., Fuente E., Montes-Morán M. A., Martin, M. J. and Linares-Solano A., 2007. A New Generation of Sludge-Based Adsorbents for H2S Abatement at Room Temperature, Environ. Sci. Technol., 41, 4375-4381.

Sarperi L., Surbrenat A., Kerihuel A., and Chazarenc F., 2014. The use of an industrial by-product as a sorbent to remove CO_2 and H_2S from biogas, J. Environ. Chem. Eng., 2, 1207-1213.

Shang G., Shen G., Liu L., Chen Q., and Xu Z., 2013. Kinetics and mechanisms of hydrogen sulfide adsorption by biochars, Bioresour. Technol., 133, 495-499.

Shang G., Li Q., Liu L., Chen P., and Huang X., 2016. Adsorption of hydrogen sulfide by biochars derived from pyrolysis of different agricultural/forestry wastes, J. Air Waste Manag. Assoc., 66, 8-16.

Sioukri E. and Bandosz T. J., 2005. Enhancement of the Performance of Activated Carbons as Municipal Odor Removal Media by Addition of a Sewage-Sludge-Derived Phase, Environ. Sci. Technol., 39, 6225-6230.

Surra E., Costa Nogueira M., Bernardo M., Lapa N., Esteves I., and Fonseca I., 2019. New adsorbents from maize cob wastes and anaerobic digestate for H_2S removal from biogas, Waste Manag., 94, 136-145.

Wallace R., Seredych M., Zhang P., and Bandosz T. J., 2014. Municipal waste conversion to hydrogen sulfide adsorbents: Investigation of the synergistic effects of sewage sludge/fish waste mixture, Chem. Eng. J., 237, 88-94.

Xiao Y., Wang S., Wu D., and Yuan Q., 2008. Catalytic oxidation of hydrogen sulfide over unmodified and impregnated activated carbon, Sep. Purif. Technol., 59, 326-332.